Available online at www.ijpe-online.com

**International Journal of Performability Engineering**

vol. 16, no. 8, August 2020, pp. 1310-1320
DOI: 10.23940/ijpe.20.08.p18.13101320

# Simulation for Target Detection in Polarimetric Scenes

Junhua Yue[a] and Yan Li[b,*]

[a]*Creative Centre for ArtSciArch, Jilin Architecture University, Changchun, 130118, China*
[b]*Changchun Institute of Optics, Fine Mechanics and Physics, Changchun, 130033, China*

**Abstract**

Aiming to precisely detect targets in complex scenes using optical remote sensing technology, the technology of modeling and simulation for polarimetric detection on remotely-sensed targets is discussed. Due to the complex interference between targets, background reflection, and aerosol radiation in real environments, the modeling and simulation of polarimetric targets are difficult. Firstly, the optical theories and basics of polarimetric model are introduced, and then a numerical simulation and analysis for Priest-Germer model are given. The Priest-Germer model obtains different results for different materials and is capable of distinguishing materials. The design idea and software frame of polarimetric detection software are provided. Finally, giving two kinds of material and two wavelength irradiation (440nm, 600nm), four groups of simulation experiments for two targets and polarimetric image histogram comparison are exhibited. The derived results prove that polarimetric simulation software based on PG model is sensitive to different targets, irradiation, and materials and provides distinguishing ability. The visualization effects are relatively good, the software has great values on practice, and it is shown that the target model, atmospheric transmission model, and physical property of materials have comprehensive and decisive effects on polarimetric imaging.

*Keywords*: polarimetric imaging; Priest-Germer model; simulation; OpenGL

(Submitted on April 12, 2020; Revised on May 22, 2020; Accepted on June 28, 2020)



## 1. Introduction

In recent years, polarization imaging technology has become a detection and identification technology [1]. It is a relatively new and immature technical field that utilizes the polarization basic attribute information (polarization degree, polarization angle, etc.) of the target scattered radiation. Even if there is no temperature difference between the two object detection points, it can be imaged by polarization contrast, which can reflect the target scene information that cannot be detected by traditional infrared detection technology [2].

In the applications of polarization remote sensing, the interaction of the scene objects can affect the polarization state of the infrared electromagnetic waves reflected or radiated on the target surface. Because the polarization detection technology has the ability to highlight the target outlines and details, it can be widely used in agricultural remote sensing and even infrared stealth and anti-stealth such as the civilian and the military fields [3]. Due to the diverse target characteristics and complex background distribution in the actual environment, it is difficult to design and implement the polarization detection system only through theoretical analysis and empirical model [4]. In order to accurately study the multi-band polarization characteristics and polarization difference laws of various targets and backgrounds, it is easy to carry out polarization detection research. As early as 2002, some countries began to study infrared polarization simulation, mainly focusing on simulation and experimental test based on the bidirectional reflectance distribution function model (BRDF) [5]. In China, some research institutes have carried out research and analysis on target characteristics, but they are still in the research stage of the polarization bidirectional reflectance distribution function pBRDF model of target base material or background material. The development of polarization simulation software has not yet been considered. In order to accurately use the polarization technology to detect targets in complex backgrounds, a multi-band polarization characteristic database of target materials is established to provide an analysis method for the study of polarization characteristics of targets in complex backgrounds.

* Corresponding author.
*E-mail address*: ly2455@sina.com

Based on the PG scattering model, this paper develops a scene target detection simulation software for polarization scenes based on the radiation data of hemispheric airspace and the physical characteristics of target materials. This paper introduces the polarization bidirectional reflectance function model, gives the Stokes expression of its polarization form, and performs numerical simulation analysis. The latest research progress on polarization detection of rough material surface targets is introduced. Meanwhile, the optical polarization information of the target models given two types of target models and two wavelength hemispheric space irradiation distributions, and two kinds of material conditions are simulated and compared through the VS2013 development platform. Finally, the polarization detection scene simulation technology is comprehensively analyzed and reviewed, and the future development trend of the technology is pointed out.

## 2. The Polarization State of Light and Its Mathematical Representation

Light has wave characteristics, and polarization is one of its basic properties. The method of combining polarization information with intensity and spectral information has important and far-reaching significance in improving the ability and accuracy of infrared detection and recognition of ground objects. In the process of light propagation, there is an infinite number of vibration directions that are perpendicular to the direction of propagation. The characteristics of vibration in different directions that are perpendicular to the direction of propagation during wave propagation is called polarization [6]. Natural light can be seen as the sum of many light waves with all possible vibration directions. Vibrations in all directions exist at the same time or replace each other quickly and irregularly. Therefore, natural light is generally considered to be unpolarized.

In general, the polarization state of light can be described using the Jones vector or Stokes vector method [6]. The Jones vector method represents the $x$ and $y$ components of the optical electric field by the Jones vector. When describing the interference effect of polarized light, the Jones vector method is easier to describe. In addition to completely polarized light, the Stokes vector can also be used to describe partially, completely unpolarized light. Its definition is expressed as follows:

$$S = \begin{pmatrix} I \\ Q \\ U \\ V \end{pmatrix} = \begin{pmatrix} E_0 + E_{90} \\ E_0 - E_{90} \\ E_{45} - E_{-45} \\ E_{RCP} - E_{LCP} \end{pmatrix} \tag{1}$$

In the above equation, $E_\theta(\theta = 0^\circ, 45^\circ, -45^\circ, 90^\circ)$ is a thermal image after rotating the polarizer at an angle of $\theta$. $E_{RCP}, E_{LCP}$ represents information on the polarization of right-handed and left-handed circles, respectively.

The Stokes vector can express the polarization information of the beam, but it has insufficient ability to describe the radiation of the target scene, the change in the polarization state of the reflection, and the relationship between the surface state of the target and its inherent properties. Two important parameters commonly used to characterize the surface state and intrinsic property of the target scene are the degree of polarization (DOP) and the angel of polarization (AOP). Through the degree of polarization, a beam of light can be expressed as a combination of completely polarized and non-polarized light, as follows:

$$S = \begin{pmatrix} DoP \cdot S_0 \\ S_1 \\ S_2 \\ S_3 \end{pmatrix} + (1 - DoP) \begin{pmatrix} S_0 \\ 0 \\ 0 \\ 0 \end{pmatrix} \tag{2}$$

Among them, the polarization of the Stokes parameter of the beam is calculated as follows:

$$Dop = \frac{\sqrt{S_1^2 + S_2^2 + S_3^2}}{S_0} \tag{3}$$

The linear degree of polarization is as follows:

$$Dolp = \frac{\sqrt{S_1^2 + S_2^2}}{S_0} \tag{4}$$

In a large number of practical infrared detection applications for remote sensing targets, the polarized light components

of the left-handed and right-handed beams reflected by the target are very weak and can be ignored. Therefore, the following formula is obtained:

$$DoP \approx DoLP = \frac{\sqrt{S_1^2 + S_2^2}}{S_0} \tag{5}$$

The polarization angle represents the polarization direction of the beam relative to the angle of the $x$-axis. For partially polarized light, it represents the angle between the polarization direction with the largest energy and the $x$-axis. The calculation formula is as follows:

$$AoP = \frac{1}{2} = arctan\left(\frac{S_2}{S_1}\right) \tag{6}$$

## 3. Polarization Model Algorithm

The reflection of the incident radiant flux by the target rough material surface and the scattering of the transmitted radiation inside the material are the two mechanisms that constitute radiation reflection. This makes the reflection coefficient of the material strongly dependent on the angle. Therefore, a bidirectional reflection distribution function (BRDF) needs to be introduced to describe the directional reflection coefficient. This function can comprehensively reflect the effect of the target surface on light waves. In the field of optical remote sensing, the bidirectional reflectance distribution function is the most widely used measurement model. In addition, the reflection characteristics of the material surface also depend on the surface texture, roughness, and other factors, and the bidirectional reflection distribution function can be more formal and accurate to the real material physical characteristics [7].

### *3.1. BRDF Model*

The bidirectional reflection distribution function model [8] (BRDF) was proposed by Nicodemus in the 1870s. The model was originally defined from the perspective of light radiation and has been greatly developed. It has been widely used in the field of laser, infrared, and microwave segments and radiation applications. It has been extended to the field of remote sensing. The bidirectional reflection distribution function represents the basic properties of optics. For a certain direction of light, the model represents the distribution of the reflected energy in the upper hemisphere [9]. Its mathematical expression is as follows:

$$f(\theta_i, \theta_i, \theta_i, \theta_i, \lambda) = \frac{dL_\gamma(\theta_\gamma, \emptyset_\gamma, \lambda)}{dE_i(\theta_i, f_\gamma, \lambda)} \tag{7}$$

In the above formula, $\theta$ represents the zenith angle in the model, $\varphi$ represents the azimuth angle in the model, and $\lambda$ indicates the wavelength of light. The measurement model and parameters of the two-way reflection distribution function are shown in Figure 1.

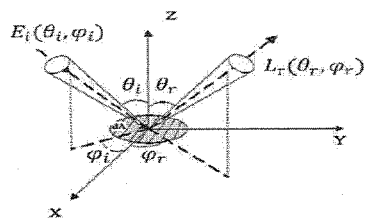


Figure 1. Bidirectional reflection distribution function model

Due to the irregularity of the rough surface of the object, we also need to introduce the micro-surface model [8] to simulate the polarization reflection characteristics of the rough surface on the computer. Without considering the multiple reflection of the light on the surface, the rough surface is decomposed into a series of tiny surface elements. Under the measurement coordinate system, the pBRDF model is applied to simulate the relationship between incident light sources, detectors, and tiny plane elements. The angular parameters and interrelationships of the rough surface micro-surface model [9] are shown in Figure 2.

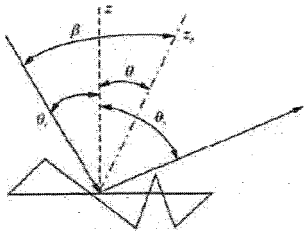

Figure 2. Micro-surface model of rough surfaces

The dotted line $Z$ is the average normal line of the rough surface, $Z_n$ is the normal direction of the microplane, $\beta$ is the angle between the incident ray and the micro-face normal, and $\theta$ is the angle between the surface average normal and the micro-face normal. According to the angular relationship of Figures 1 and 2, $\theta$ and $\beta$ can be calculated by the following formula:

$$cos\,2\beta = cos\,\theta_i + sin\,\theta_i\,sin\,\theta_\gamma\,cos(\emptyset_\gamma - \emptyset_i) \tag{8}$$

$$\theta = arc\,cos\left(\frac{cos\,\theta_i + cos\,\theta_\gamma}{2\,cos(\beta)}\right) \tag{9}$$

At present, there are three kinds of BRDF models that are widely used in the field of optical remote sensing at home and abroad: the Torrance-Sparrw BRDF (TS model), Beard-Maxwell BRDF (BM model), and Priest-Gemmer BRDF (PG model). The TS model is a physics-based analysis model that uses radiometrics and micro-surface theory to derive high-light reflection models of rough. It mainly considers the material physical characteristics of the material surface and texture roughness. The BM model is a statistical model. Sampling points are dense and the amount of data is very large, so the BM model is not suitable for real-time fields. The PG model is an empirical model and an effective combination of the TS model and the BM model. It is not based on physical principles, but rather presents empirical formulas that simulate lighting by adjusting parameters. The PG model introduces the Mueller matrix to represent the Fresnel scattering effect of the material surface based on the previous two models, and it can represent the Stokes vector of scattered light [8, 10]. Therefore, this paper mainly introduces the PG model and performs infrared polarization scene simulation for this model.

### *3.2. PG Model*

The PG (Priest-Germer) model [8, 11] is an empirical model that uses Fresnel reflection theory model for rough surface material reflection. The distribution of reflected energy in the upper hemisphere is based on empirical models of statistics. It is an extension of Torrans-Sparrw BRDF and Beard-Maxwell BRDF. It can measure and simulate the polarization state changes after light is reflected on the material surface. The model itself is a polarizing form of the bidirectional reflection distribution function (polarizing BRDF). In addition, DIRSIG (digital and remote sensing image simulation software developed by the University of Rochester, USA) also uses the PG model as the core model and has greater theoretical and practical value in the field of national defense engineering and industrial applications.

PG model reflection calculation usually includes three parts: mirror reflection, non-polarization body scattering, and diffuse scattering. Actually, the body scattering will also have a small effect on the overall polarization state of the reflected light. The PG model treats body scattering as completely non-polarized information. In practice, body scattering also has a small impact on the overall polarization state of reflected light. The general form of the reflection calculation of the model is as follows:

$$f_{pBRDF} = f_{spec} + f_{vol} = f_{polarized} + f_{urpolarized} \tag{10}$$

$$f_{spec} = \frac{M(\beta, n, k)SO(\theta, \beta, \tau, \Omega)}{4\,cos(\theta_i)\,cos(\theta_\gamma)} \tag{11}$$

$$f_{vol} = \rho_d + \frac{2\rho_v}{cos(\theta_i) + cos(\theta_\gamma)} \tag{12}$$

The calculation of the specular reflection part of the model is mainly based on the statistical distribution of the Fresnel reflection matrix function. In addition, the shadow and occlusion functions are introduced in the PG model, which further approaches the actual light reflection.

The specular reflection calculation part changes the polarization state of the reflected light. The main factor is a 4 × 4 Mueller matrix [9-10]. The PG model mainly uses the reflection coefficient and phase delay angle of the p and s waves to calculate the Mueller matrix of the conductor. Obtain the following matrix form:

$$M = \frac{1}{2}\begin{pmatrix} r_s^2 + r_p^2 & r_s^2 + r_p^2 & 0 & 0 \\ r_s^2 + r_p^2 & r_s^2 + r_p^2 & 0 & 0 \\ 0 & 0 & 2r_s r_{p\cos\Delta} & -2r_s r_{p\sin\Delta} \\ 0 & 0 & 2r_s r_{p\sin\Delta} & 2r_s r_{p\cos\Delta} \end{pmatrix} \tag{13}$$

$r_s$ and $r_p$ are the reflection coefficients of the s-wave and the p-wave in the equations, respectively, and $\Delta$ is the phase delay angle. According to Fresnel's law, the following parameters are calculated:

$$r_s = -\frac{sin(\theta_i - \theta_t)}{sin(\theta_i + \theta_t)} \tag{14}$$

$$r_p = -\frac{tan(\theta_i - \theta_t)}{tan(\theta_i + \theta_t)} \tag{15}$$

$$\Delta = \emptyset_s - \emptyset_p \tag{16}$$

$$sin(\theta_i) = (n + ik)\, sin\, \theta_t \tag{17}$$

Since the rough material surface we encounter is not ideally smooth in the real simulation environment, the PG model introduces a small bin probability distribution function $P_{G/C}(\theta, \sigma, B)$. The basic idea of this function is to use the micro-face normal and material averaging method. The angle of the line is used to characterize the relationship between the intensity of the reflected light and the slope of the surface of the material. The commonly used distribution function forms a Gaussian distribution and Cauchy distribution, as follows:

$$P_G(\theta, \sigma, \beta) = \frac{\beta e^{\left(\frac{tan\,\theta^2}{2\sigma^2}\right)}}{2\pi\sigma^2\, cos(\theta)^3} \tag{18}$$

$$P_G(\theta, \sigma, \beta) = \frac{\beta}{cos(\theta)\,(\sigma^2 + tan(\theta)^3)} \tag{19}$$

The parameter $B$ in the formula represents the deviation of the micro-face normal distribution, and the parameter $\sigma$ represents the mean square error of the slope of the micro-face in a specific area of the rough surface. In order to further approach the real situation, the PG model introduces a shadow and occlusion function $SO(\theta, \beta, \tau, \Omega)$, which mainly simulates the shadow and occlusion effects of the surface of the rough material on the reflected light [8]. The shadowing effect and masking effects to light on rough material are shown in Figure 3.

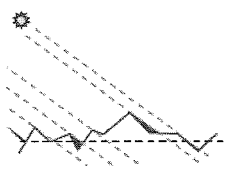

Figure 3(a). Shadowing effects to light on rough surfaces

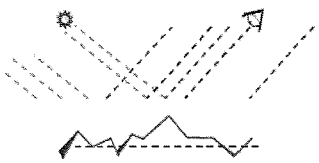

Figure 3(b). Masking effects to light on rough surfaces

The effective shadow and occlusion functions that most widely used are based on the ideas in the Beards-Maxwell BRDF

model, and they are implemented and applied in the NEF database. The function form is as follows:

$$SO(\theta,\beta,\tau,\Omega) = \frac{1+\frac{\theta}{\Omega}}{1+\frac{\theta}{\Omega}} e^{(-\beta/\tau)} \tag{20}$$

The parameter $\beta$ is the specular reflection angle of the ray relative to the normal of the micro-element, and the parameters $\tau$ and $\Omega$ are shadow and mask function parameters. The smaller the values of $\tau$ and $\Omega$, the larger the surface roughness of the material, and the stronger the shadowing effect, so that the oblique incident light and the scattered light have a relatively greater possibility of being blocked by other micro-facets or reflected again in other directions.

In addition to calculating the specular polarization effect of the Fresnel form, the PG model also takes into account the non-polarized scattering components of light. The non-polarized component includes two parts of full scattering and bulk scattering, and the calculation method is as follows:

$$f_{vol} = \rho_d + \frac{2\rho_v}{cos(\theta_i) + cos(\theta_i)} \tag{21}$$

The diffuse scattering parameter $\rho_d$ simulates the ideal scattering of the Lambertian body, which is independent of the scattering direction and completely unpolarized. The bulk scattering parameter $\rho_v$ characterizes the effect of incident irradiance absorbed by the micro-element and is immediately reflected out. The bulk scatter is also completely unpolarized [10].

## 4. PG Model Analysis and Numerical Simulation

The PG model simulation needs to set the coordinate system calculated by the model. The plane where the panel is located is the *x*-*y* plane, the *y*-axis points to the azimuth angle of 0 degrees, the clockwise is [0, +180] degrees, the counterclockwise is [0, -180] degrees, the *z*-axis points to the zenith angle of 0 degrees, and from the *z*-axis to the xy-horizontal plane is the zenith angle [0, +90] degrees, as shown in Figure 4.

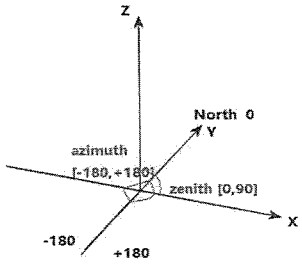


Figure 4. Coordinate system of PG

The incident orientation of the incident light is fixed below, and two different material parameters are selected to perform numerical simulation analysis on all the detection directions of the hemisphere airspace. The model parameters are detected as a horizontal angle of [-180, +180] degrees and an azimuth angle of [0, +90] degrees, and numerical simulation results are calculated at intervals of 1 degree. We can conclude that the material 1 micro-surface probability distribution function reaches a maximum value of 270 in the azimuth $\pm 180^{\circ}$ and pitch angle $45^{\circ}$, while the material 2 micro-surface probability distribution function reaches a maximum value of 0.22 in the vicinity of the azimuth $\pm 180^{\circ}$ and pitch angle $60^{\circ}$. The shadow and occlusion functions for material 1 and material 2 are shown in Figure 5.

It can be seen that material 1 has a maximum value 1 of the shadow and occlusion function when the azimuth angle $\pm 180^{\circ}$, $0^{\circ}$ and the pitch angle $45^{\circ}$, and the function is symmetrically distributed with respect to the azimuth angle of 0 degrees and the elevation angle of 45 degrees. Material 2 has a maximum value 1 of the shadow and occlusion function when the azimuth angle $\pm 180^{\circ}$, $0^{\circ}$ and the pitch angle $60^{\circ}$. The difference between the shadow and occlusion function of the two materials is different. The S0 strength values corresponding to azimuth and zenith of materials 1 and 2 are shown in Figure 6. The DOP values corresponding to azimuth and zenith of materials 1 and 2 are shown in Figure 7.

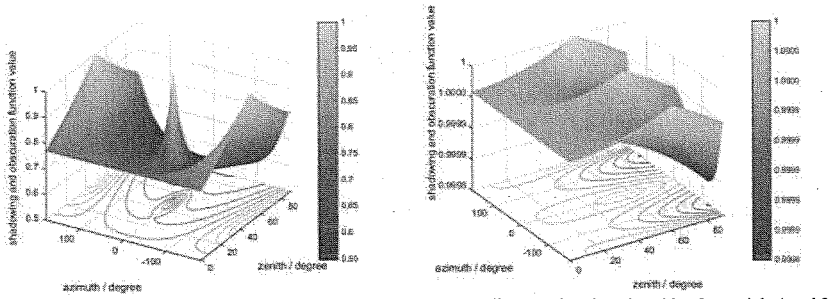


Figure 5. Shadowing and obscuration function value corresponding to azimuth and zenith of materials 1 and 2

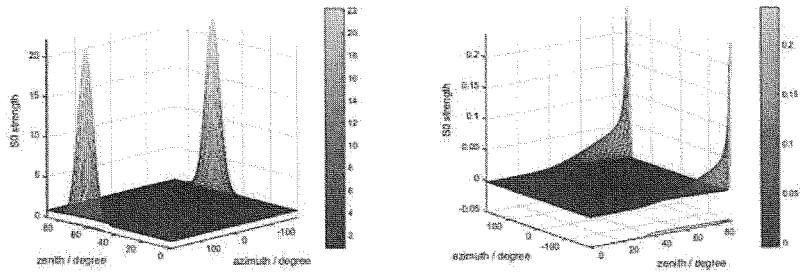


Figure 6. S0 strength value corresponding to azimuth and zenith of materials 1 and 2

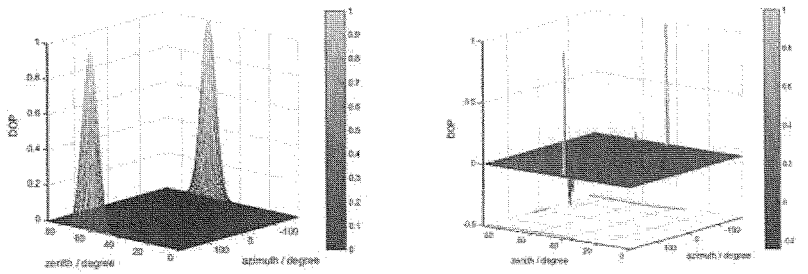


Figure 7. DOP value corresponding to azimuth and zenith of materials 1 and 2

It can be seen that the scattering intensity and polarization of material 1 and material 2 are different from the general trend of the detection orientation, and the range of extreme values is also different. In summary, it can be concluded that the detection simulation using PG model can obtain different numerical results for different materials, and different simulation results can also be obtained for different observation directions [11].

## 5. Simulation Software Design and Simulation Results

The simulation software development platform is mainly based on the VS2013 integrated development environment and the development language C/C++. The simulation software can demonstrate better visualization effects. The pre-development 3D scene model combination and calibration were implemented using Autodesk 3ds Max 2012. After the software reads the scene model and the sky hemisphere airspace model file, it dynamically optimizes the hemispheric airspace irradiation model, then calculates each surface element of the scene model based on the PG model, and iteratively obtains the polarization simulation data of all the microelements of the target model. Finally, the polarization simulation results of the scene model are rendered interactively to the display interface using OpenGL. The software processing process is shown in Figure 8.

The simulation calculation of the polarization scene mainly depends on the PG model. Before the calculation, it is necessary to set the model parameters of the material. The different optical characteristic parameters of the material will change with the irradiation light of different wavelengths. The common PG model material (green paint, black paint) parameters are shown in Table 1.

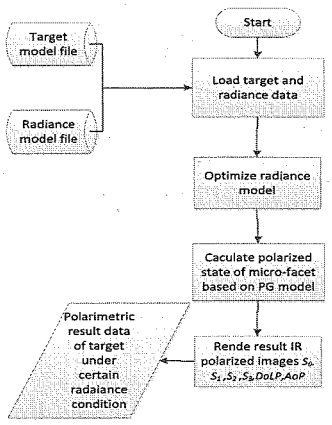


Figure 8. Flow diagram of simulation software

Table 1. PG model parameters for rough materials surface (green paint, black paint)

| Material | $\lambda$/nm | $n$ | $k$ | $B$ | $\sigma$ | $\tau$ | $\Omega$ | $\rho_d$ | $\rho_V$ |
|---|---|---|---|---|---|---|---|---|---|
| Green Paint | 440 | 1.3766 | 0.28959 | 0.173996 | 0.468383 | 0.22121 | 1.68383 | 0.042161 | 0.001769 |
| | 550 | 1.366 | 0.2746 | 0.0235 | 0.1288 | 8.789e1 | 1.499e2 | -9.450e-4 | -1.285e-3 |
| | 600 | 1.125 | 1.000 | 0.0068 | 0.0742 | 1.471e2 | 5.338e1 | 4.108e-3 | -1.645e-3 |
| Black Paint | 440 | 1.4330 | 0.0102 | 0.5742 | 0.8524 | 4.756e1 | 7.410e-2 | 2.290e-2 | 3.100e-2 |
| | 550 | 1.2850 | 0.2923 | 0.2356 | 0.8057 | 7.145e1 | 1.960e-1 | 1.664e-3 | 6.500e-3 |
| | 600 | 1.7730 | 0.4146 | 0.0706 | 0.7556 | 2.286e2 | 2.092e0 | 6.629e-4 | 2.812e-4 |

The polarization scene simulation software needs to set the polarization light distribution data of the hemispheric airspace. In the simulation experiment, 440nm and 600nm atmospheric polarization light distribution under clear weather conditions are selected as simulation experimental data. The atmospheric polarization light distribution data for both bands is shown in Figure 9. The S3 component of atmospheric polarization light in two bands is negligible. The atmospheric polarization light distribution of the two wavelengths is similar, and the numerical intensity is different.

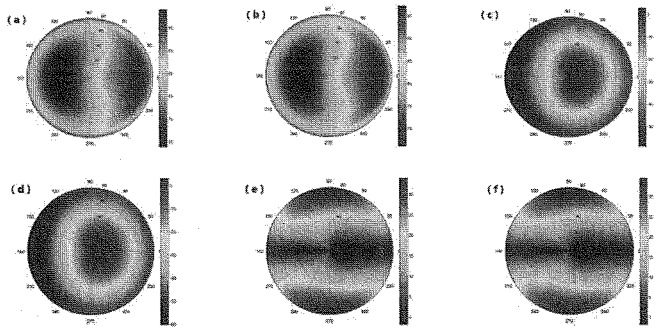


Figure 9. Polarimetric light distribution of atmosphere: (a) 440nm S0; (b) 600nm S0; (c) 440nm S1; (d) 600nm S1; (e) 440nm S2; (f) 600nm S2

The simulation results of the polarization scenes of the two types of targets (target A and target B, respectively) in the 440nm and 600nm bands are given below, and the corresponding gray histogram characteristic curves are given.

The first set of simulation experiments: The target A surface material is set with green paint material, and the probability distribution model of the surface surface of the microelement is set to Gaussian distribution. The detector is at an azimuth angle of 0 degrees and a zenith angle of 30 degrees. The histograms of the simulation results of the radiation wavelengths are shown in Figure 10.

The second set of simulation experiments: The surface material of the target A is set with black lacquer material, and the

surface probability distribution model of the micro-face element is set to Gaussian distribution. The histograms of the simulation results of the two groups of irradiated wavelengths at an azimuth angle of 0 degrees and a zenith angle of 30 degrees are shown in Figure 11.

The third group of simulation experiments: The target B surface material is set with green paint material, the surface probability distribution model is set to Gaussian distribution, and the detector has an azimuth angle of 0 degrees and a zenith angle of 30 degrees. The histograms of the simulation results are shown in Figure 12.

The fourth group of simulation experiments: The surface material of the target B is set with black lacquer material, and the surface probability distribution model of the micro-face element is set to Gaussian distribution. The detector is at an azimuth angle of 0 degrees and a zenith angle of 30 degrees. The histograms of the simulation results of the irradiation wavelengths are shown in Figure 13. The experimental results show that the same target in the same material and different wavelengths of radiation will produce different polarization images, mainly because the same material will show different physical properties and intensity at different wavelengths. The S0 image is different from the DOP image.

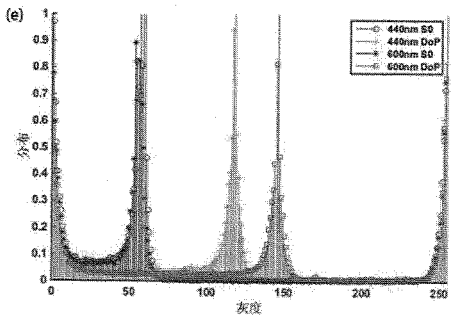


Figure 10. The histograms of simulation result of test 1

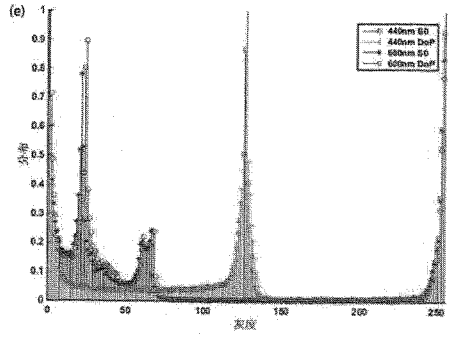


Figure 11. The histograms of simulation result of test 2

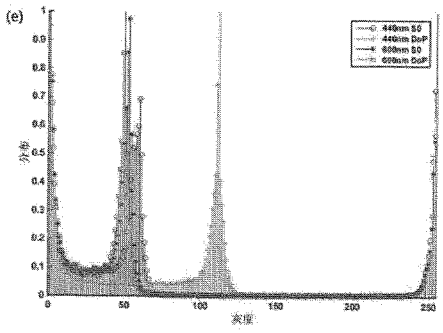


Figure 12. The histograms of simulation result of test 3

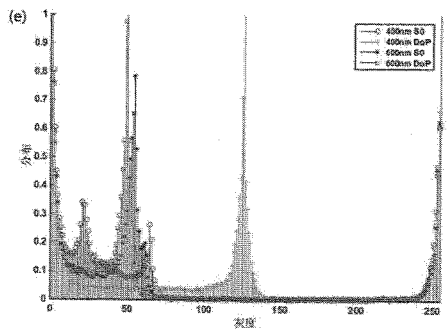


Figure 13. The histograms of simulation result of test 4

The histograms of different material strength contrast diagrams of target A in 440 nm wavelength of Experiment 1 and Experiment 2 were compared, as shown in Figure 14. The histograms of the DOP images under the 440 nm irradiation of Experiment 1 and Experiment 2 were compared, as shown in Figure 15. From the comparison results of the above two groups, the polarization result images generated by the same target under the same wavelength irradiation condition will change according to different materials, and the grayscale distribution area of the image is different. The material can be distinguished according to the grayscale distribution model.

The S0 polarization results of Experiment 1 and Experiment 3 under 400nm and 600nm irradiation conditions were compared, respectively shown as Figures 16 and Figure 17.

From the above two comparisons, the grayscales of the S0 polarization images of different targets under the same material irradiation conditions are similar but not identical, mainly because the surface micro-element distributions of different targets

are different, and the probability distribution function pairs in the PG model are different. The target has different effects, and thus the polarization simulation algorithm can distinguish different targets.

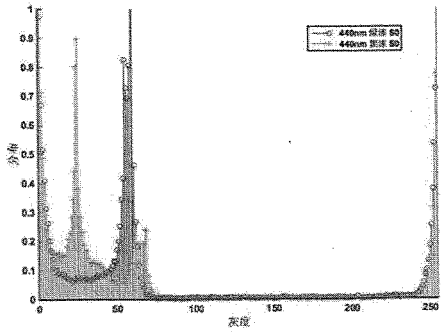


Figure 14. Different material strength contrast diagrams in 440nm wavelength

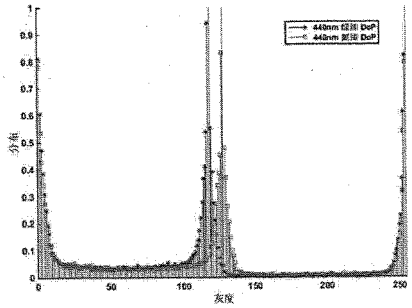


Figure 15. Different material DoP contrast diagrams in 440nm wavelength

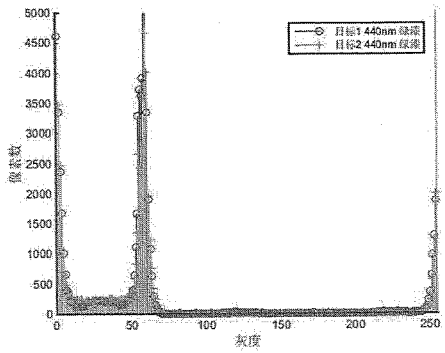


Figure 16. Contrast of S0 polarization image in 440 nm irradiation

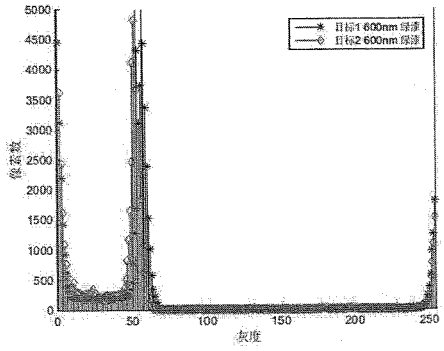


Figure 17. Contrast of S0 polarization image in 600 nm irradiation

Based on the four groups of experiments and the above comparison results, it can be seen that the simulation results based on the PG model depend on different atmospheric irradiation conditions (irradiation wavelength), physical properties of different materials, and bin distribution characteristics of the target surface. Specifically, different targets have different grayscale distribution histograms of the simulation results under the same irradiation environment and the same material condition, the same target has different simulation results under the same material and different irradiation environment conditions, and the same target is in the same radiation. The simulation results are different according to the environment and different materials.

It is concluded that the polarization simulation software based on the PG model has high sensitivity to targets, irradiation, and material, and it can provide better resolution and recognition ability. It compares the polarization state image, which can be highlighted by using a gray histogram. The difference between the polarization state images facilitates the estimation of the target based on the grayscale distribution histogram. In addition, simulation software based on the VS (C++) platform can achieve more intuitive visualization.

## 6. Conclusion

In this paper, the simulation effects of the PG model under different targets, different materials, and different irradiation backgrounds are studied. A visual and interactive polarization scene simulation method is proposed and implemented. In order to distinguish the target, the function of generating grayscale map of polarized images is provided. The overall simulation effects of the polarization scene target detection simulation are good and applicable, which provides an objective reference and solution for future agricultural remote sensing, geographic information, and war simulation. The simulation results effectively show that the use of optical remote sensing polarization information can effectively detect targets and distinguish materials. This technology is receiving more and more attention, and researchers are also optimizing and innovating existing technologies.

The next work of this project will be based on the basic material rough panel physical polarization image and polarization software generated by the target polarization image to achieve the purpose of model verification. From the current technical development trend, the next research direction of simulation implementation process is the further consideration of the secondary scattering relationship between the background and the target. In addition, in order to obtain the polarization scene simulation results faster and more accurately, the development direction of the application of the technology is the optimization of the irradiation model and the target polarization state calculation algorithm.

## References


1. Q. Liu, Y. H. Zhan, and D. Yang, "Parameters of the Polarimetric Bidirectional Reflectance Distribution Function of Rough Surfaces and Parameters Inversion," *Journal of Spacecraft TT&C Technology*, Vol. 34, No. 5, pp. 481-488, 2015
2. J. Duan, Q. Fu, C. H. Mo, et al., "Research on Military Applications of Polarization Imaging in Foreign Countries," *Journal of Infrared Technology*, Vol. 10, No. 3, pp. 190-195, 2014
3. M. Gao, C. Song, and L. Gong, "Analysis of Polarization Characteristics about Rough Surface Light Scattering based on Polarized Bidirectional Reflectance Distribution Function," *Journal of Chinese Lasers*, Vol. 40, No. 12, pp. 12-13, 2013
4. K. Tang, J. W. Zhou, T. Jiang, et al., "Research on Infrared Polarization Characteristics of Target and Background," *Journal of Infrared and Laser Engineering*, Vol. 36, No. 5, pp. 611-614, 2007
5. J. F. Tao, X. P. Sheng, and Q. Sun, "Analysis of Near-Field Scattering Characteristics of Complex Targets," *Journal of Modern Radar*, Vol. 27, No. 10, pp. 75-78, 2006
6. W. L. Chen, S. H. Wang, W. Q. Jin, and J. W. Li, "Research of Infrared Polarization Characteristics based on Polarization Micro-surface Theory," *Journal of Infrared Millimeter Waves*, Vol. 33, No. 5, pp. 507-514, 2014
7. M. W. Hyde IV, J. D. Schmidt, and M. J. Havrilla, "A Geometrical Optics Polarimetric Bidirectional Reflectance Distribution Function for Dielectric and Metallic Surfaces," *Journal of Optics Express*, Vol. 17, No. 24, pp. 22151, 2009
8. R. G. Priest and T. A. Germer, "Polarimetric BRDF in the Micro-Facet Model: Theory and Measurements," in *Proceedings of the 2000 Meeting of the Military Sensing Symposia Specialty Group on Passive Sensors*, pp. 169-181, Ann Arbor, January 2000
9. Q. Li, Z. J. Liu, B. J. Shu, et al., "Target Recognition Technology using Polarization Difference of Surface Scattered Light," *Journal of Strong Laser and Particle Beam*, Vol. 17, No. 3, pp. 351-354, 2005
10. B. S. Zhang, W. Q. Liu, Q. N. Wei, et al., "Analysis of Target Scattering Characteristics based on Experimental Measurement of Bidirectional Reflection Distribution Function," *Journal of Optical Technology*, Vol. 32, No. 1, pp. 180-182, 2006
11. R. G. Priest and S. R. Meier, "Polarimetric Microfacet Scattering Theory with Applications to Absorptive and Reflective Surface," *Journal of Optical Engineering*, Vol. 41, No. 5, pp. 988-993, 2012


**Junhua Yue** is an associate associate professor at Jilin Architecture University. Her research interests include digital image processing and pattern recognition.

**Yan Li** is a researcher in fine mechanics and physics at the Changchun Institute of Optics. His research interests include pattern recognition and visual simulation technology.